

GA-A24337

**CURRENT DRIVE AND PRESSURE PROFILE
MODIFICATION WITH ELECTRON CYCLOTRON
POWER IN DIII-D QUIESCENT DOUBLE BARRIER
EXPERIMENTS**

by

**T.A. CASPER, K.H. BURRELL, E.J. DOYLE, P. GOHIL, C.M. GREENFIELD,
R.J. GROEBNER, R.J. JAYAKUMAR, M.A. MAKOWSKI, T.L. RHODES,
and W.P. WEST**

JULY 2003

DISCLAIMER

This report was prepared as an account of work sponsored by an agency of the United States Government. Neither the United States Government nor any agency thereof, nor any of their employees, makes any warranty, express or implied, or assumes any legal liability or responsibility for the accuracy, completeness, or usefulness of any information, apparatus, product, or process disclosed, or represents that its use would not infringe privately owned rights. Reference herein to any specific commercial product, process, or service by trade name, trademark, manufacturer, or otherwise, does not necessarily constitute or imply its endorsement, recommendation, or favoring by the United States Government or any agency thereof. The views and opinions of authors expressed herein do not necessarily state or reflect those of the United States Government or any agency thereof.

**CURRENT DRIVE AND PRESSURE PROFILE
MODIFICATION WITH ELECTRON CYCLOTRON
POWER IN DIII-D QUIESCENT DOUBLE BARRIER
EXPERIMENTS**

by

**T.A. CASPER,* K.H. BURRELL, E.J. DOYLE,[†] P. GOHIL, C.M. GREENFIELD,
R.J. GROEBNER, R.J. JAYAKUMAR,* M.A. MAKOWSKI,* T.L. RHODES,[†]
and W.P. WEST**

This is a preprint of a paper to be presented at the 30th European Physical Society Conference on Controlled Fusion and Plasma Physics, St Petersburg, Russia, July 7-11, 2003 and to be published in the *Proceedings*.

*Lawrence Livermore National Laboratory, Livermore, California.

[†]University of California at Los Angeles, Los Angeles, California.

**Work supported by
the U.S. Department of Energy
under Contract Nos. DE-AC03-99ER54463, W-7405-ENG-48 and
Grant No. DE-FG03-01ER54615**

**GENERAL ATOMICS PROJECT 30033
JULY 2003**

Current Drive and Pressure Profile Modification with Electron Cyclotron Power in DIII-D Quiescent Double Barrier Experiments

T.A. Casper¹, K.H. Burrell², E.J. Doyle³, P. Gohil², C.M. Greenfield², R.J. Groebner²,
J. Jayakumar¹, M.A. Makowski¹, T.L. Rhodes³, W.P. West²

¹Lawrence Livermore National Laboratory, P.O. Box 808, Livermore, California 94551
USA

²General Atomics, P.O. Box 85608, San Diego, California 92186-5608 USA

³University of California, Los Angeles, Box 951597, Los Angeles, California 20742 USA

High confinement mode (H-mode) operation is a leading scenario for burning plasma devices [1,2] due to its inherently high energy-confinement characteristics. The quiescent H-mode (QH-mode [3,4]) offers these same advantages with the additional attraction of more steady edge conditions where the highly transient power loads due to edge localized mode (ELM) activity is replaced by the steadier power and particle losses associated with an edge harmonic oscillation (EHO) [3-5]. With the addition of an internal transport barrier (ITB), the capability is introduced for independent control of both the edge conditions and the core confinement region giving potential control of fusion power production for an advanced tokamak configuration. The quiescent double barrier (QDB) [3-8] conditions explored in DIII-D experiments exhibit these characteristics and have resulted in steady plasma conditions for several confinement times ($\sim 26 \tau_E$) with moderately high stored energy, $\beta_{NH89} \sim 7$ for $10 \tau_E$.

More recent QDB experiments on DIII-D [7,8] have been aimed at using these moderately high β steady plasma conditions to explore the possibility for current profile control using electron-cyclotron heating (ECH) and current drive (ECCD). These experiments, motivated by transport modeling to explore the effects of ECH and ECCD, were consistent with the modeling predictions and provided an initial demonstration of the effects of current profile control in the DIII-D tokamak. As a result of this direct ECCD, we observed significant changes in the q-profile both near the EC resonance location and at the magnetic axis due to inductive effects. In addition to the current profile modification predicted, we also observed a reduction in the density profile peaking and an associated beneficial reduction in the total impurity concentration. This modification of the density profile resulted in secondary changes in the current profile both through changes in the neutral-beam-driven current (NBCD) and self-consistent changes in the bootstrap current. In these counter-NBCD discharges, we observe a narrowing of the neutral-beam current profile resulting from a change in neutral-beam deposition due to changes in the electron temperature profile from heating and the density profile from changes in transport. We observed offsetting changes in the bootstrap current that was expected to increase with heating but was ultimately reduced by large changes in the local density gradient as the profile peaking is reduced. These profile-induced changes in current drive complicate the evolution of the q profile and its subsequent control but afford the opportunity for simultaneous control of q, pressure and impurities. In this paper, we discuss details of the current profile modification observed.

Formation of the QDB conditions in DIII-D requires establishment of two distinct and separate barrier regions, an ITB that forms near $\rho \sim 0.5$ and an edge barrier region outside $\rho \sim 0.95$ where ρ is the square root of the toroidal flux coordinate. A region of higher transport due to a change in the polarity of the $E \times B$ shearing rate [5] maintains this separation of core and edge barrier regions. To date, we have only been successful in achieving this configuration with counter-injected neutral beams (NBCD opposite to the Ohmic current). Using early counter-neutral-beam injection and divertor pumping, we achieve the QDB conditions indicated in Fig. 1. These parameters are typical of shots used in these EC current profile control experiments. Neutral-beam power is increased after formation of the QDB conditions at 1.5 s to achieve higher stored energy. With the presence of an ITB, a moderate pressure peaking of $p/\langle p \rangle \sim 2.5$ is achieved but locally steep gradients may be limiting β_N . We produce quiescent and nearly steady-state plasmas with durations limited by the available neutral-beam pulse length. Predictive transport [7] simulations using these conditions explored the heating and current drive effects expected from injecting microwave power resonant at $2\omega_{CE}$, 110 GHz in DIII-D. In these experiments, we observed a significant modification of the q profile at the onset of EC power as evidenced by the drop in q_{\min} [Fig. 1(d)]. The early rapid drop in q_{\min} results from a redistribution of currents due to establishment of ECCD and prompt changes in the pressure profile. In concert with the onset of EC power, we observe a change in particle confinement exhibited by a reduction in the line-average density, Fig. 1(h), and in the density peaking as shown in Fig. 2(a) along with the calculated ECCD from TORAY-GA [9,10]. This change in density profile is accompanied by a significant reduction in both the carbon and high-Z, Cu and Ni, impurities, Fig. 1(i,j) [7,8]. The total thermal plus fast-ion pressure also changes but to a lesser amount. For a given radial resonance location, these changes in the density profiles are insensitive to the EC antenna aiming for current drive or radial launch. Increases in the electron temperature, Figs. 1(e) and 2(b), resulting from ECH are consistent with expectations from transport modeling using the TORAY-GA code. We observe the ion temperature to decrease during EC power

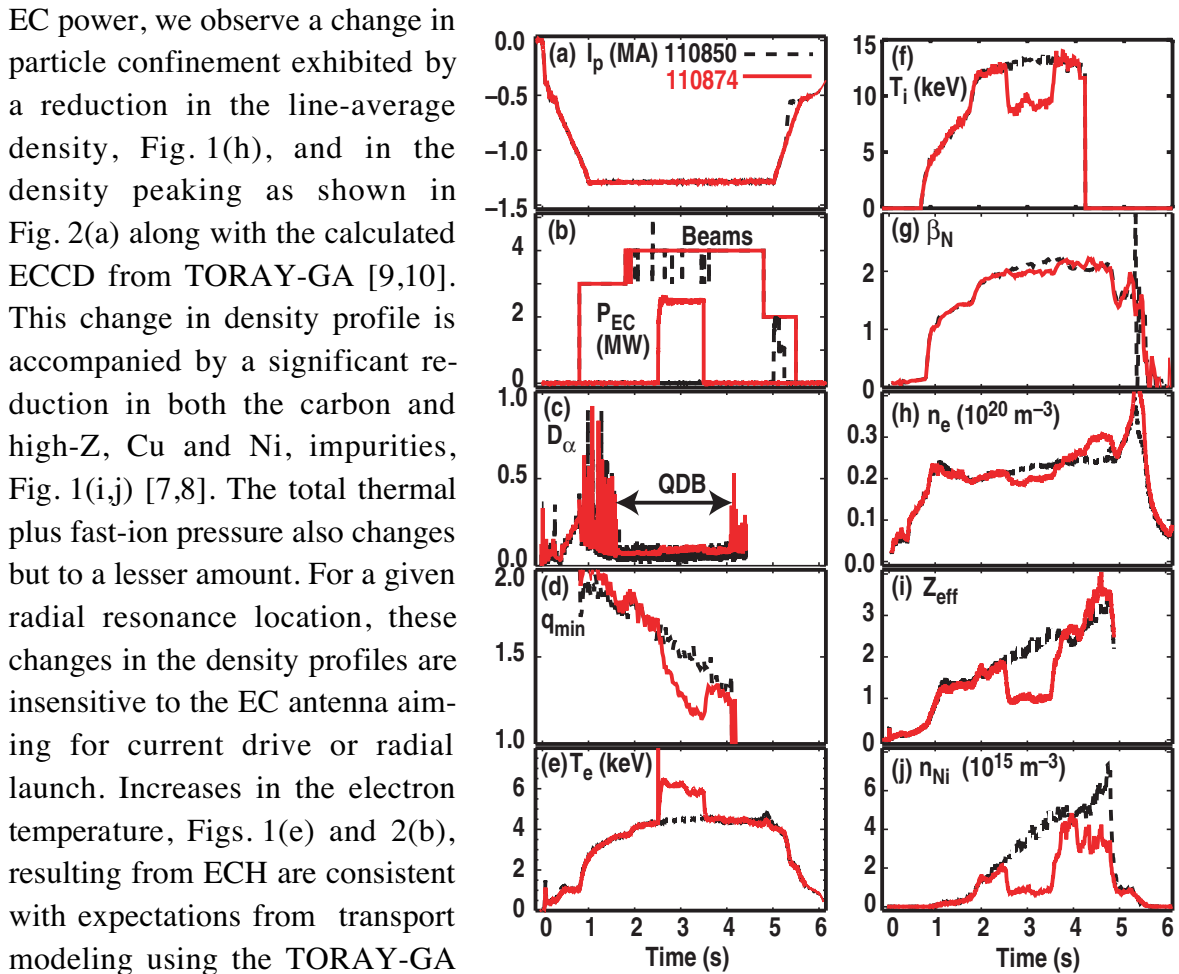


Fig. 1. QDB parameters for no ECCD reference 110850 and shot 110874 with 2 MW EC power with co-ECCD aiming at $\rho = 0.2$.

injection, Fig. 1(f). The rising T_e accompanied by falling T_i and n_e result in a small reduction in stored energy and are indicated by β_N in Fig. 1(g). These changes result in a reduction of the overall bootstrap current drive along with changes in the neutral beam deposition and current drive.

We show in Fig. 3 the effect on the various current drive components for co-ECCD conditions (along Ohmic current) with 2 MW of power injected to heat and drive current near $\rho \sim 0.2$. Since we cannot measure the individual noninductive current drive components, of necessity we must assess the current drive components using a model-based approach with NBCD determined from NFREYA [11] plus a fast ion orbit model, ECCD from Toray-GA and bootstrap current drive from NCLASS [12]. In this assessment, we use a time-sequence of measured density and temperature profiles from the experiment (no thermal or particle transport model assumed) and Ohm's law using the calculated noninductive current drive components to determine the time-changing equilibrium from a solution to the Grad-Shafranov equation using Corsica's equilibrium solver [13,14]. The rapid drop in the density profile near the magnetic axis results in greater peaking of the NBCD, Fig. 3(a), due to additional penetration of the neutral beams thus moving the deposition closer to the magnetic axis. The possibility of additional changes in the NBCD due to fast ion orbit effects resulting from changes in the local magnetic field have not yet been determined. The bootstrap current decreases in time, Fig. 3(a), since the density gradient drive in the bootstrap model dominates over increases expected from the electron heating. These density-profile-induced changes in the NBCD and the bootstrap current are insensitive to the EC antenna aiming, radial launch or current drive direction, and complicate the evolution of the q-profile and our ability to control it and determine the current profile response inside the EC resonance. The minimum of q, q_{min} , is reduced as we show in Fig. 3(c) by a combination of direct ECCD current profile modification near the current drive location,

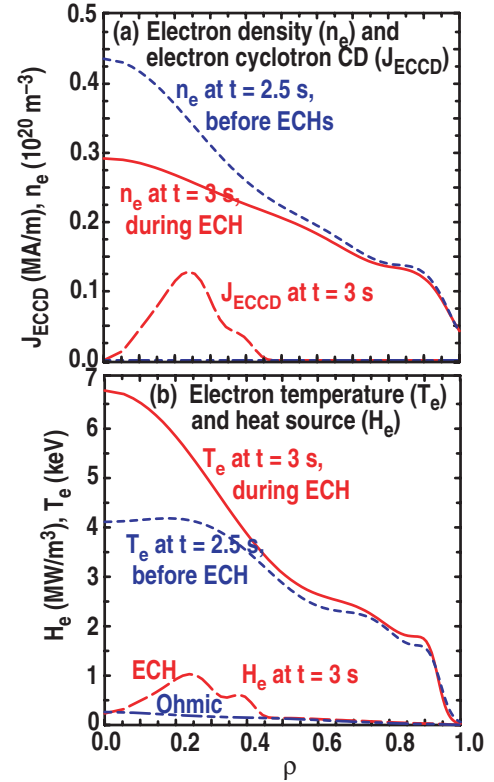


Fig. 2. Density and temperature profile response to EC power inside barrier.

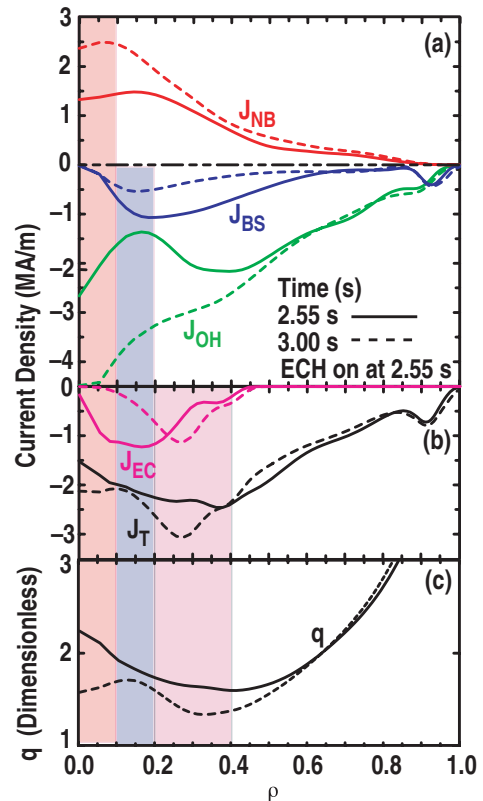


Fig. 3. Current and q profile response to EC injected inside the ITB for shot 110874 with 2 MW EC for co-ECCD at $\rho = 0.2$.

Fig. 3(b), and the combined, spatially and temporally dependent effects of the NBCD and bootstrap current. The overall effect is to drive q_{\min} down as expected from predictive simulations while modifying the magnetic shear near the magnetic axis as determined from the total parallel current shown in Fig. 3(b). That this effect is occurring is indicated in Fig. 4 where we show a comparison of the calculated MSE synthetic diagnostic signals with the raw data acquired for this shot from the MSE channels viewing the region near the magnetic axis. We note the reasonably good comparison of the time evolution of the synthetic and real MSE signals that indicates our calculated current profile evolution from the analysis of this shot is substantially correct.

In summary, by injecting 2 MW of EC power with antennas aimed for ECCD along the Ohmic current, we were able to significantly modify the local minimum value of q and change the magnetic shear near the magnetic axis inside the EC resonance. Injection of EC power inside the ITB heated the electrons as expected but also significantly altered the density profiles for electrons and impurities, changing the density peaking factor $n_e/\langle n_e \rangle$ from 2.1 to 1.5. This change in density resulted in modification to both the local bootstrap and neutral beam current drive

components that, in turn, also modified the local q profile. This synergistic modification of the current profile will complicate development of q -profile control capabilities for these ITB discharges. However, in addition to current profile control, it also affords the possibility for directly changing the density, pressure and impurity profiles for control of the barrier and possibly of β -limits as well. In this first experiment, we obtained some preliminary data indicating our ability to increase T_i and β through the use of feedback on the neutral beam power during ECCD that will be pursued in future experiments.

This work was supported by the U.S. Department of Energy under contracts DE-AC03-99ER54463, W-7405-ENG-48, and grant DE-FG03-01ER54615.

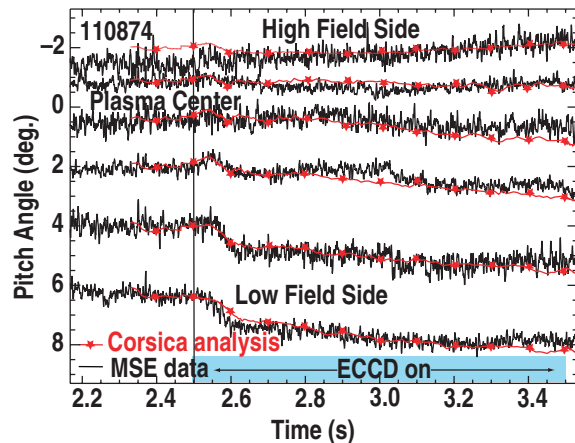


Fig. 4. Comparison of MSE data and calculated synthetic MSE data from evolution of current profiles and equilibrium.

- [1] ITER Physics Basis Document, Nucl. Fusion **39**, 2137 (1999).
- [2] Taylor, T.S., Plasma Phys. Controlled Fusion **39**, B47 (1997).
- [3] Burrell, K.H., *et al.*, Phys. Plasmas **8**, 153 (2001).
- [4] Doyle, E.J., *et al.*, Plasma Phys. and Control. Fusion **43**, A95 (2001).
- [5] Greenfield C.M., *et al.*, Phys. Rev. Lett. **20**, 4544 (2001).
- [6] Greenfield, C.M., *et al.*, Plasma Phys. and Control. Fusion **44**, A123 (2002).
- [7] Casper, T.A., *et al.*, Proc. 29th EPS Conf. on Controlled Fusion and Plasma Physics, Montreux, Switzerland, 2002.
- [8] Doyle, E.J., *et al.*, 19th IAEA Fusion Energy Conf., Lyon, France, 2002, EX/C3-2.
- [9] Cohen, R.H., *et al.*, Phys. Fluids **30**, 2442 (1987).
- [10] Lin-Liu, Y.R., *et al.*, Radio Frequency Power in Plasmas (Proc. 12th Topical Conf., CP403 (195) 1997).
- [11] Goldston, R.J., *et al.*, J. Comp. Physics **43**, 61 (1981).
- [12] Houlberg, W.A., *et al.*, Phys. Plasmas **4**, 3230 (1997).
- [13] LoDestro, L.L. and Pearlstein, L.D., Phys. Plasmas **1**, 90 (1994).
- [14] Pearlstein, L.D., *et al.*, Proc. 28th EPS Conf. on Controlled Fusion and Plasma Physics, Madeira, Portugal, 2001.